Journal of Catalysis 257 (2008) 125–133

Contents lists available at ScienceDirect

Journal of Catalysis

www.elsevier.com/locate/jcat

Good sulfur tolerance of a mesoporous Beta zeolite-supported palladium catalyst in the deep hydrogenation of aromatics

Tiandi Tang, Chengyang Yin, Lifeng Wang, Yanyan Ji, Feng-Shou Xiao *

College of Chemistry and State Key Laboratory of Inorganic Synthesis and Preparative Chemistry, Jilin University, Changchun 130023, PR China

ARTICLE INFO

Article history:
Received 26 January 2008
Revised 9 April 2008
Accepted 20 April 2008
Available online 21 May 2008

Keywords:
Mesoporous Beta zeolite
Palladium catalyst
Naphthalene
Pyrene
Hydrogenation
Sulfur tolerance
4,6-Dimethyldibenzothiophene
Hydrodesulfurization

ABSTRACT

The activities of a Pd catalyst supported on mesoporous Beta zeolite (Beta-H) were evaluated for the hydrogenation of naphthalene and pyrene in the absence and presence of 200-ppm sulfur and for the hydrodesulfurization (HDS) of 4,6-dimethyldibenzothiophene (4,6-DMDBT). Compared with Pd/Al-MCM-41, the Pd/Beta-H catalyst exhibited better sulfur tolerance for hydrogenation of naphthalene and pyrene and higher activity for HDS of 4,6-DMDBT. The ratio of the hydrogenation of the second ring naphthalene in the absence and presence of 200-ppm sulfur for Pd/Beta-H was larger than that for Pd/Al-MCM-41 (0.47 vs 0.19). The desulfurization effect of Pd/Beta-H was greater than that of Pd/Al-MCM-41 (51 vs 35%). The difference in sulfur tolerance and HDS ability of the 2 catalysts is attributed to the difference in support acidity. Beta-H exhibited more acidic sites and a higher percentage of strong acidic sites than Al-MCM-41 (552 μmol/g and 43% vs 291 μmol/g and 18%).

1. Introduction

The high content of aromatics in diesel fuels lowers the fuel quality [1,2]. One solution to this problem is deep hydrogenation of aromatics at low temperature over supported noble metal catalysts [1–3]. However, the presence of sulfur strongly influences the catalytic activity in deep hydrogenation due to the poisoning of active sites [4,5]. Therefore, a deep hydrogenation catalyst with good sulfur tolerance is highly desirable [2,3].

It has been reported that the catalytic activity and sulfur tolerance in deep hydrogenation of aromatic hydrocarbons can be enhanced by noble metals on acidic supports, such as HY [6–8], Beta [9], and LTL [10] zeolites. This phenomenon is attributed to the partial electron transfer from the metal particles to the acidic sites of zeolitic supports [1,11], and to the fact that electron-deficient metal particles have a better resistance to sulfur poisoning with decreased interaction with H_2S [5]. Another explanation for the improved activity of metal particles on acidic supports is the creation of a second hydrogenation pathway by spillover of hydrogen atoms from the metal particles to the aromatic sulfur-containing molecules that are adsorbed on acidic sites in the vicinity of the metal particles [12–14]. While the metal particles become poisoned by sulfur, they can be recovered from the hydrogenation pathway by spillover hydrogen [15–17].

Despite their advantages, however, conventional zeolites cannot accomplish deep hydrogenation of the bulky aromatics in diesel fuels, due to their pore size limitations [18–21]. Recently, mesoporous zeolites, such as Beta and MFI, have been successfully synthesized [22–25]. These mesoporous zeolites exhibit excellent catalytic properties for the conversion of bulky molecules. In particular, palladium catalysts supported on mesoporous Beta zeolite show superior performance in deep hydrogenation of bulky aromatic pyrene [21]. In the present work, we demonstrate that a palladium catalyst supported on strongly acidic and hierarchically mesoporous Beta zeolite (Pd/Beta-H) has a good sulfur tolerance in the deep hydrogenation of polyaromatics such as relatively small naphthalene and bulky pyrene. In contrast, palladium catalysts supported on conventional acidic zeolites cannot convert bulky pyrene. These features are very important for increasing fuel quality and controlling the undesirable emissions in exhaust gases.

Usually, deep hydrogenation of aromatics over supported noble metal catalysts is carried out at low temperatures after hydrodesulfurization (HDS) of the fuels over metal sulfide catalysts such as sulfided CoMo and NiMo supported on γ-alumina under severe operating conditions. Generally, after HDS, the sulfur molecules remaining in the fuels are mainly refractory dialkyldibenzothiophenes, such as 4,6-dimethyldibenzothiophene (4,6-DMDBT) [2,26–29], due to the steric hindrance of the methyl groups present at the 4 and 6 positions [30–32].

It has been suggested that an improvement in the acidity in the catalyst support is favorable for the HDS of 4,6-DMDBT [33–40].

* Corresponding author. Fax: +86 431 85168624.
E-mail address: fsxiao@mail.jlu.edu.cn (F.-S. Xiao).

0021-9517/$ – see front matter
doi:10.1016/j.jcat.2008.04.013

Typical catalyst supports for HDS are γ-alumina and amorphous aluminosilicates [1–3,41,42]. Acidic zeolites added to the alumina-supported CoMo and NiMo catalysts enable dealkylation and isomerization reactions of the alkyl substituents, which may transform refractory 4,6-DMDBT into more reactive species and thus accelerate HDS [33,34]. On the other hand, although zeolites have much stronger acidity than γ-alumina and amorphous aluminosilicates, the relatively small pore size of zeolites strongly hinders the mass transport of the relatively large 4,6-DMDBT molecule (8.7×12.2 Å) [43,44]. In the present work, we investigated the possibility of sulfur removal by the conversion of 4,6-DMDBT at mild reaction conditions (250 °C and 6.5 MPa) over Pd/Beta-H. In contrast, conventional HDS catalysts such as CoMo/γ-Al_2O_3 are used under relatively severe operating conditions.

2. Experimental

2.1. Catalysts

Beta-H and Al-MCM-41 were synthesized as described in the literature [22,45]. The H-form of the samples was ion-exchanged twice with a NH_4NO_3 solution (1 M) at 80 °C for 3 h, followed by calcination at 550 °C for 4 h. The Beta-H and Al-MCM-41 supported palladium catalysts were prepared by the ion-exchange method as described previously [21], with palladium loadings of 3.1 wt% for Pd/Beta-H and 3.4 wt% for Pd/Al-MCM-41, as determined by the inductively coupled plasma method (ICP; Perkin-Elmer 3300 DV). The Pd/Beta-H and Pd/Al-MCM-41 catalysts were calcined in flowing oxygen (150 mL/min, STP) from room temperature to 450 °C at a heating rate of 1 °C/min, and then held at 450 °C for 100 min.

2.2. Characterization

Nitrogen physisorption was carried out using a Micromeritics ASAP 2010M system. Before the measurement, the sample was degassed for 10 h at 300 °C. The pore size distribution was calculated using the BJH model. The acidities of the Beta-H and Al-MCM-41 were determined using the stepwise temperature-programmed desorption of ammonia [21].

The calcined Pd/Beta-H and Pd/Al-MCM-41 samples for transmission electron microscopy (TEM) were reduced by mixed H_2–N_2 gas with 6% H_2, similar to the reduction procedure in the hydrogenation test. The used Pd/Beta-H catalyst was also observed after the pyrene hydrogenation reaction. The TEM images were obtained on a JEOL JSM-3010 electron microscope operating at 300 kV.

The palladium dispersion on the supported catalysts was estimated from dynamic CO chemisorption measurements. In a typical run, about 130 mg of calcined sample was reduced in flowing mixed H_2–N_2 gas with 6% H_2 (40 mL/min STP) from room temperature to 300 °C at a heating rate of 2 °C/min and then held at 300 °C for 100 min. After reduction, the catalyst was purged with He (99.999%, 40 mL/min STP) at 290 °C for 2 h to eliminate chemisorbed hydrogen, followed by cooling to 30 °C in a He flow. Subsequently, 100 µL of CO was injected to the reduced catalyst at 10-min intervals by the pulse method until saturation adsorption was observed. The estimated dispersion and average particle size of the palladium particles are based on spherical geometry and an adsorption stoichiometry of CO/Pd = 1. The average Pd particle size was calculated by the following equation [46]:

$$d = 1.1289/D,$$

where d and D represent palladium particle size (in nm) and dispersion, respectively.

X-ray photoelectron spectroscopy (XPS) of reduced catalysts was performed using a Thermo ESCA LAB 250 system. The calcined catalyst was reduced in a mixed H_2–N_2 gas with 6% H_2 (60 mL/min, STP) from room temperature to 300 °C at a heating rate of 2 °C/min and held at 300 °C for 100 min. After reduction, the catalyst was purged with N_2 (99.999%, 60 mL/min STP) at 290 °C for 1 h. After being cooled to room temperature, the reduced catalyst was transferred under nitrogen stream into a bottle filled with absolute alcohol. For XPS, the alcohol in the bottle was removed, and the residual reduced catalyst was quickly moved to the sample holder, then transferred into the analysis chamber of the XPS instrument, followed by evacuation [43].

2.3. Activity tests

The hydrogenation of naphthalene (5 g) was carried out in an autoclave using dodecane (120 mL) as the solvent with 330 mg of catalyst at 240 °C. Hydrogenation of pyrene (3.5 g) was carried out in an autoclave using tridecane (120 mL) as the solvent with 300 mg of catalyst at 250 °C. Hydroisomerization of decalin (4.5 mL) was carried out in an autoclave using dodecane (120 mL) as the solvent with 330 mg of catalyst at 240 °C. The sulfur tolerance in the deep hydrogenation of naphthalene and pyrene was studied in the presence of thiophene and 4,6-DMDBT (200-ppm sulfur). Hydrodesulfurization of 4,6-DMDBT (0.2 g, 95% purity) was carried out using tridecane (110 mL) as the solvent with 300 mg of catalyst at 250 °C. In these reactions, the total pressure was 6.5 MPa (hydrogen pressure of about 6.2 MPa), and the stirring rate was 800 rpm. To maintain the same total pressure, hydrogen was continually supplied to make up for the consumption of hydrogen in the reaction. The reaction products were analyzed with an Agilent 6890N gas chromatograph equipped with a flame ionization detector and a mass spectrometer (TRACE MS). The Parr 5500 autoclave had a volume of 300 mL. In a typical run, the calcined catalyst powder (<53 µm) was reduced in flowing mixed H_2–N_2 gas with 6% H_2 (80 mL/min, STP) from room temperature to 300 °C at a heating rate of 2 °C/min and held at 300 °C for 100 min. After being cooled to room temperature, the reduced catalyst was transferred under nitrogen stream into the autoclave filled with solvent and reactant. In these reactions, the absence of mass diffusion limitation was checked by changing the catalyst granule size and stirring rate.

3. Results and discussion

3.1. Catalyst characterization

Table 1 presents textural parameters and acidic properties of the various supports and catalysts. Notably, after the loading of Pd particles, the surface area, mesopore volume, and micropore volume were reduced, due to the Pd particles inside the mesopores and micropores. In addition, Beta-H and Pd/Beta-H showed a wide mesopore size distribution of about 5–40 nm (Figs. 1a and 1b), and Al-MCM-41 and Pd/Al-MCM-41 exhibited narrow mesopores of about 2.3 nm (Figs. 1c and 1d). Beta-H exhibited more acidic sites than Al-MCM-41. For the characterization of acidity by NH_3-TPD, the acidic strength can be differentiated as weak, middle, and strong according to the desorption temperature [47]. Beta-H had higher concentrations of relatively strong (250–350 °C, 234 µmol/g) and strong (>350 °C, 237 µmol/g) acidic sites compared with Al-MCM-41 (105 and 53 µmol/g, respectively, Table 1).

Fig. 2 shows TEM images of the samples. The Pd particles were located in both disordered mesopores (Fig. 2b; particle size about 5 nm) and ordered micropores (insert in Fig. 2b; particle size <1 nm) of Pd/Beta-H, which is consistent with the fact that the Beta-H sample contains both hierarchical mesopores (5–40 nm) and ordered micropores (0.7 nm). After pyrene hydrogenation, the TEM images of the Pd/Beta-H catalyst showed that the Pd particles were still located in the mesopores and micropores of the sample

Table 1
Textural and acidic parameters of the samples

Samples	BET surface area (m^2/g)	External surface area[a] (m^2/g)	Mesoporous volume (cm^3/g)	Microporous volume (cm^3/g)	Acidic amounts of the support (μmol/g)			
					150–250 °C	250–350 °C	>350 °C	Total
Beta-H	524	151	0.24	0.17	81	234	237	552
Pd/Beta-H	466	134	0.21	0.15				
Al-MCM-41	799	–	0.62	–	133	105	53	291
PdAl-MCM-41	721	–	0.54	–				

[a] Mesoporous surface area is included.

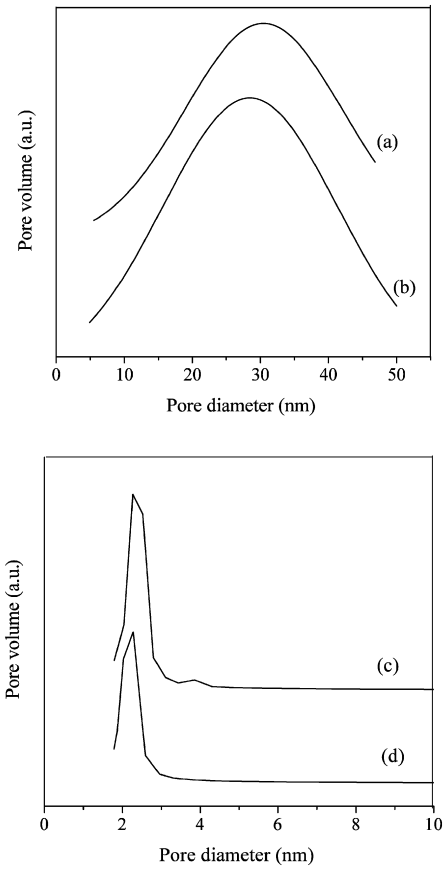

Fig. 1. Pore size distribution curves of (a) Beta-H, (b) Pd/Beta-H, (c) Al-MCM-41, and (d) Pd/Al-MCM-41.

(Fig. 2c), suggesting that the Pd particles in Beta-H did not readily aggregate in pyrene hydrogenation. In the Pd/Al-MCM-41 catalyst, the Pd particles were located mainly in mesopore channels of Al-MCM-41, with an average particle size of about 2.2 nm (Fig. 2d).

Table 2 presents the results of XPS and CO chemisorption of Pd/Beta-H and Pd/Al-MCM-41. The binding energies of the Pd $3d_{5/2}$ peak of Pd/Beta-H (335.5 eV) and Pd/Al-MCM-41 (335.0 eV) clearly differed (Fig. 3), suggesting that Pd clusters on Pd/Beta-H were electron-deficient compared with those on Pd/Al-MCM-41. This is due to the close contact between the strong acid site and the small cluster of Pd atoms, which allows withdrawal of electrons from the noble metal, creating an electron-deficient metal particle [5,11]. Furthermore, estimation of Pd particle size by CO chemisorption showed average Pd particle sizes of 2.4 nm on Beta-H and 2.2 nm on Al-MCM-41.

3.2. Naphthalene hydrogenation

Fig. 4 shows the proposed network of naphthalene hydrogenation. The hydrogenation of naphthalene occurs in two steps: the conversion to tetralin, followed by the formation of decalin [48].

Table 2
XPS and CO-chemisorption data over Pd/Beta-H and Pd/Al-MCM-41 catalysts

Catalysts	Pd loading (wt%)	Binding energy Pd $3d_{5/2}$ (eV)	CO-chemisorption	
			CO/Pd	*d* (nm)
Pd/Beta-H	3.1	335.5	0.47	2.4
Pd/Al-MCM-41	3.4	335.0	0.52	2.2

Naphthalene hydrogenation can be basically considered an irreversible pseudo-first-order consecutive reaction under a pressure >3.1 MPa and a reaction temperature <275 °C, the second step being the slow step [48]. In our case, the reaction pressure was 6.5 MPa and the reaction temperature was 240 °C; therefore, naphthalene hydrogenation was considered an irreversible pseudo-first-order consecutive reaction.

Fig. 5 illustrates the time dependence of naphthalene conversion over the Pd/Beta-H and Pd/Al-MCM-41 catalysts. Notably, the activities of Pd/Beta-H and Pd/Al-MCM-41 were quite different for the conversion of tetralin to decalin; for example, after reaction for 180 min, this conversion was 82% over Pd/Beta-H but only 20% over Pd/Al-MCM-41. The conversion of naphthalene to tetralin at 240 °C was close to 100% over both catalysts; however, when the reaction temperature was decreased to 200 °C, this conversion (at 80 min of reaction time) dropped to 92% over Pd/Beta-H and 66% over Pd/Al-MCM-41. These results indicate that Pd/Beta-H had greater hydrogenation activity than Pd/Al-MCM-41 catalyst in naphthalene hydrogenation.

Fig. 6 shows the time dependence of naphthalene conversion over the Pd/Beta-H and Pd/Al-MCM-41 catalysts in the presence of 200-ppm sulfur in the form of thiophene. Compared with the results in Fig. 5, here the catalytic activity in the hydrogenation of naphthalene to tetralin over Pd/Beta-H was hardly influenced by the addition of 200-ppm sulfur, but the same amount of sulfur resulted in a significant reduction of the catalytic activity over Pd/Al-MCM-41. Furthermore, the catalytic activity in the hydrogenation of tetralin to decalin was significantly suppressed over both Pd/Beta-H and Pd/Al-MCM-41 by the presence of 200-ppm sulfur, but the poisoning effect was much stronger over Pd/Al-MCM-41 than over Pd/Beta-H; for example, at a reaction time of 180 min, the conversion of tetralin to decalin was 46% for Pd/Beta-H, compared with only 3% for Pd/Al-MCM-41. These results indicate that Pd/Beta-H had a much better sulfur tolerance in the hydrogenation of naphthalene compared with Pd/Al-MCM-41.

Table 3 presents the product selectivity in naphthalene hydrogenation over Pd/Beta-H and Pd/Al-MCM-41 in the absence and presence of 200-ppm sulfur in the form of thiophene for a reaction time of 60 min. Compared with Pd/Al-MCM-41, Pd/Beta-H exhibited much higher activity for the conversion of tetralin and selectivity for decalins in the absence and presence of 200-ppm sulfur (runs 1–4).

We also analyzed the byproducts of naphthalene hydrogenation. We found no byproducts for Pd/Al-MCM-41 but found several byproducts for Pd/Beta-H, including octahydro-2,5-dimethylpentalene, 1-butyl-cyclohexene, 1-butyl-cyclohexane, and light hydrocarbons (C_5–C_9). This suggests that hydrocracking of naphthalene occurred over Pd/Beta-H. After 60 min, the selectivity

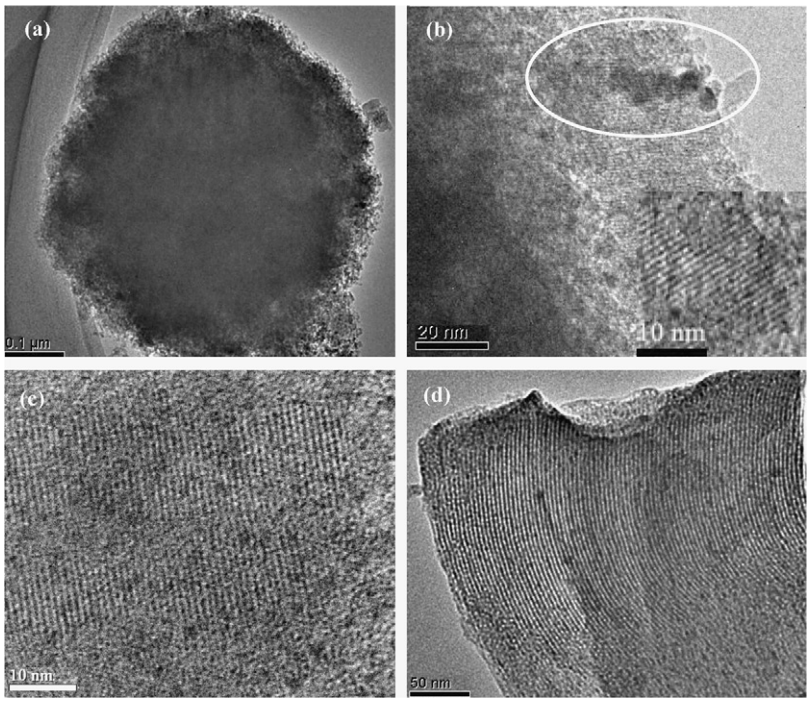

Fig. 2. TEM images of Pd/Beta-H and Pd/Al-MCM-41 catalysts. (a) Large-scale TEM image of the reduced Pd/Beta-H, (b) high resolution TEM images of the reduced Pd/Beta-H, (c) high resolution TEM image of the used Pd/Beta-H, (d) the reduced Pd/Al-MCM-41. Insert in (b): TEM image of Pd particles in micropores.

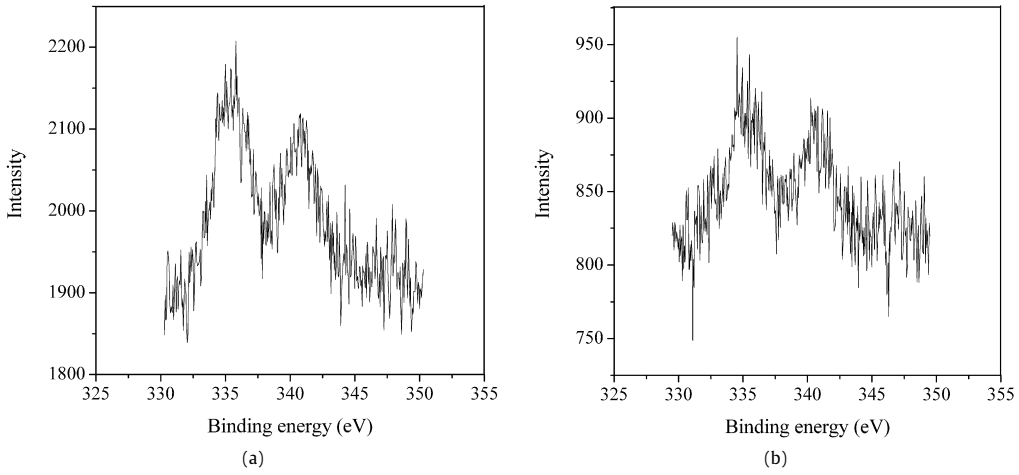

Fig. 3. XPS spectra of (a) Pd/Beta-H and (b) Pd/Al-MCM-41catalysts.

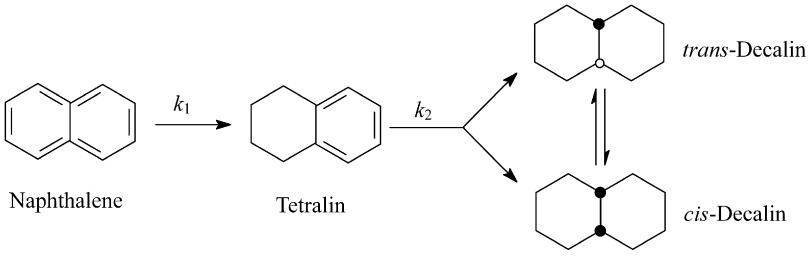

Fig. 4. Network of naphthalene hydrogenation.

for byproducts was 4.6% (run 1 in Table 3); when the reaction time was increased to 180 min, the selectivity for byproducts reached 25%. The formation of byproducts from hydrocracking may be associated with strongly acidic sites on the Pd/Beta-H catalyst.

To carefully compare sulfur tolerance, we estimated the rate constants derived with the pseudo-first-order assumption for the hydrogenation of the second ring of naphthalene in the absence (k_{2c}) and presence (k_{2s}) of thiophene [43,48] over Pd/Beta-H and Pd/Al-MCM-41 (Table 4). The rate constants were normalized to per mol of metal atoms. Both k_{2s} and k_{2s}/k_{2c} for Pd/Beta-H were much higher than those for Pd/Al-MCM-41, confirming the better sulfur tolerance of Pd/Beta-H. The different sulfur tolerance in

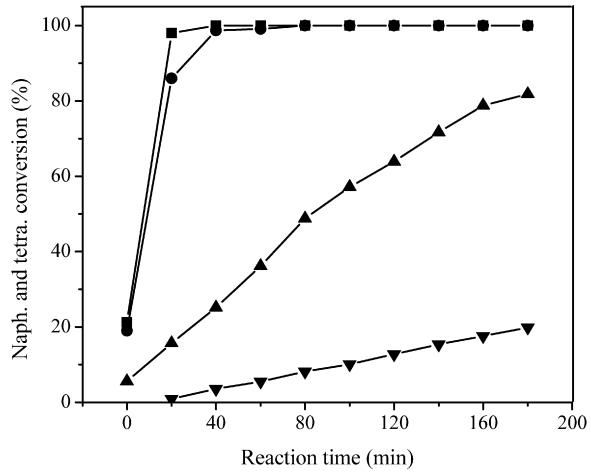

Fig. 5. Dependence of the naphthalene and tetralin conversion on reaction time in the absence of thiophene. (■) Naphthalene conversion over Pd/Beta-H; (●) naphthalene conversion over Pd/Al-MCM-41; (▲) tetraline conversion over Pd/Beta-H; (▼) tetralin conversion over Pd/Al-MCM-41.

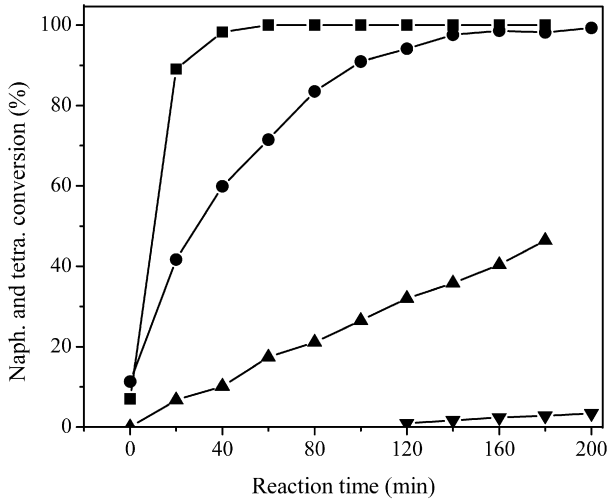

Fig. 6. Dependence of the naphthalene and tetralin conversion on reaction time in the presence of 200-ppm sulfur in the form of thiophene. (■) Naphthalene conversion over Pd/Beta-H; (●) naphthalene conversion over Pd/Al-MCM-41; (▲) tetraline conversion over Pd/Beta-H; (▼) tetralin conversion over Pd/Al-MCM-41.

these two catalysts may be due to their different acidities; similar phenomena have been reported previously [6–10]. The close contact between the strong acidic sites and the small clusters of palladium may cause withdrawal of electrons from the palladium atoms, thereby creating electron-deficient palladium particles, which decreases the bond strength between the electron acceptor, such as sulfur, and the electron-deficient palladium [5,11]. This explanation is supported by the change in the binding energy of Pd $3d_{5/2}$ for Pd/Beta-H (335.5 eV) and Pd/Al-MCM-41 (335.0 eV) (Table 2), in good agreement with those reported by other groups [5,43,48]. Cooper and Donnis [5] proposed that the close contact between the strong acidic sites and the small clusters of Pt and Pd atoms allows withdrawal of electrons from the noble metal, thereby creating an electron-deficient metal particle. Meng et al. [43] reported a greater binding energy of Pd $3d_{5/2}$ on strongly acidic HY zeolite (335.5 eV) than on weaker acidic HUSY zeolite (335.1 eV). Their catalytic tests in naphthalene hydrogenation showed that the Pd/HY sample was more active than the PdPt/HUSY sample in the presence and absence of thiophene. Corma et al. [48] reported that small Pt clusters were localized in the supercages of the USY zeolite and were subjected to greater

Table 3
Product selectivities in naphthalene hydrogenation over Pd/Beta-H and Pd/Al-MCM-41 catalysts for reaction time of 60 min

Run	Catalyst	Tetralin conversion (%)	Product selectivity (%)				
			Tetralin	*t*-Decalin	*c*-Decalin	By-product	Total decalins
1	Pd/Beta-H	36.3	63.7	17.2	14.5	4.6	31.7
2	Pd/Beta-H[a]	17.4	82.6	8.3	7.3	1.8	15.6
3	Pd/Al-MCM-41	5.5	94.5	3.2	2.4	0	5.6
4	Pd/Al-MCM-41[a]	0	71.5	0	0	0	0

[a] The presence of 200-ppm sulfur in the form of thiophene.

Table 4
Comparison of the rate constants of the hydrogenation of the second ring of naphthalene over Pd/Beta-H and Pd/Al-MCM-41 in the absence and presence of 200-ppm sulfur in the form of thiophene

Catalysts	k_2 (L/mol$_M$ h)		
	k_{2c}	k_{2s}	k_{2s}/k_{2c}
Pd/Beta-H	521	243	0.47
Pd/Al-MCM-41	92	18	0.19

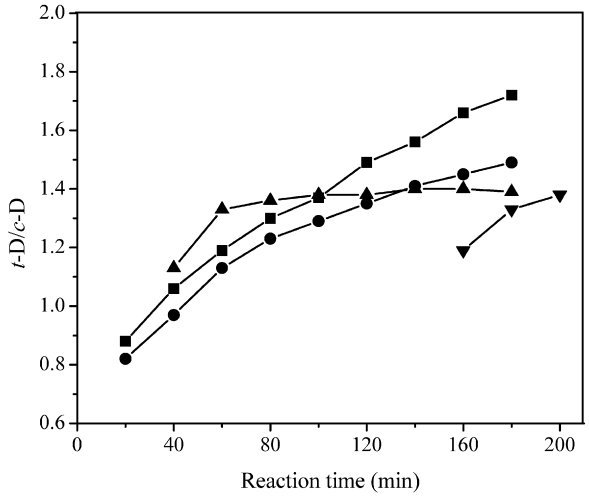

Fig. 7. Dependence of the ratio of *trans*-decalin/*cis*-decalin in naphthalene hydrogenation on reaction time in the absence and presence of 200-ppm sulfur in the form of thiophene. (■) In the absence of thiophene over Pd/Beta-H; (●) in the presence of thiophene over Pd/Beta-H; (▲) in the absence of thiophene over Pd/Al-MCM-41; (▼) in the presence of thiophene over Pd/Al-MCM-41.

interaction with the strongly Brönsted acidic sites of the zeolite to form electron-deficient Pt particles of enhanced hydrogenation activity and improved sulfur tolerance. In this work, the Beta-H zeolite with strong and abundant acidic sites (which also could make the electrons withdraw from the palladium atoms) resulted in good sulfur tolerance in naphthalene hydrogenation.

Fig. 7 illustrates the time dependence of the *trans*-decalin/*cis*-decalin (*t*-D/*c*-D) ratio during naphthalene hydrogenation over Pd/Beta-H and Pd/Al-MCM-41. For Pd/Al-MCM-41, the ratio of *t*-D/*c*-D quickly reached a constant value of 1.3–1.4 in the absence of sulfur. In contrast, the ratio of *t*-D/*c*-D over Pd/Beta-H increased with reaction time in the absence and presence of 200-ppm sulfur. This phenomenon is attributed to the isomerization of *cis*-decalin to *trans*-decalin on the Pd/Beta-H, which was further confirmed by the hydroisomerization of pure decalin (Fig. 8). Comparing Figs. 7 and 8 shows a *t*-D/*c*-D close to 1.7 in naphthalene hydrogenation over Pd/Beta-H for a reaction time of 180 min, compared with the 8.8 in hydroisomerization, indicating the suppression of hydroisomerization by the presence of naphthalene and tetralin. Huang and Kang [49] also reported that the presence of tetralin in naphthalene hydrogenation strongly limited the conversion of *c*-decalin to *t*-decalin.

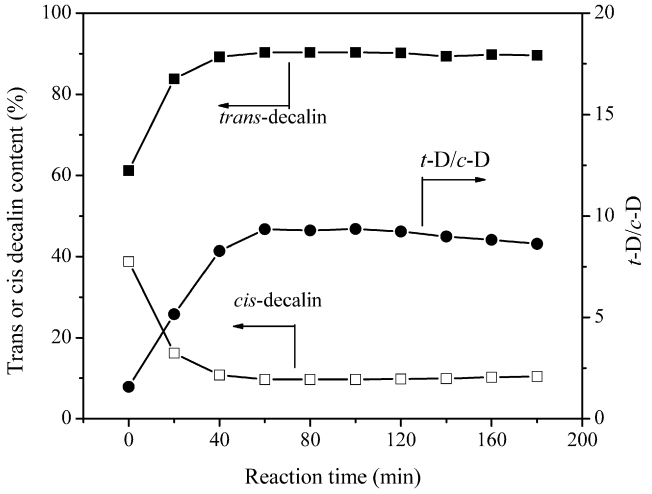

Fig. 8. Dependence of *trans*-decalin and *cis*-decalin content and *trans*-decalin/*cis*-decalin ratio in decalin hydroisomerization on reaction time over Pd/Beta-H. (■) *Trans*-decalin content; (□) *cis*-decalin content; (●) *trans*-decalin/*cis*-decalin ratio.

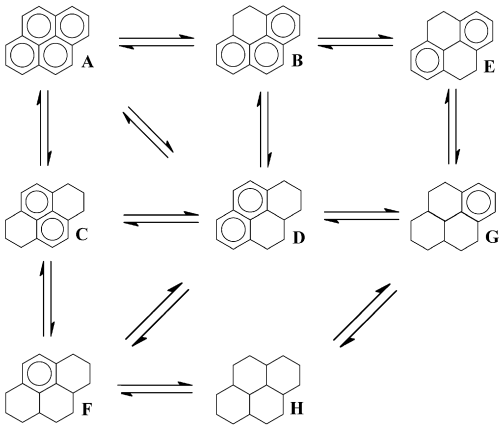

Fig. 9. The proposed network of pyrene hydrogenation. (A) Pyrene; (B) 4,5-dihydropyrene; (C) 1,2,3,6,7,8-hexahydropyrene; (D) 1,2,3,3a,4,5-hexahydropyrene; (E) 4,5,9,10-tetrahydropyrene; (F) 1,2,3,3a,4,5,5a,6,7,8-decahydropyrene; (G) 1,2,3,3a,4,5,9,10,10a,10b-decahydropyrene; (H) perhydropyrene.

3.3. Pyrene hydrogenation

Fig. 9 shows the proposed network of pyrene hydrogenation [21]. Pyrene hydrogenation is a consecutive reaction that first creates dihydropyrene, followed by the formation of tetrahydropyrene, hexahydropyrene, decahydropyrene, and perhydropyrene [21].

Fig. 10 illustrates the time dependence of pyrene conversion over Pd/Beta-H and Pd/Al-MCM-41 in the absence and presence of thiophene. Obviously, the conversion of pyrene over the two catalysts was significantly reduced by the addition of 200-ppm sulfur in the form of thiophene, but the suppression of the catalytic activity over Pd/Al-MCM-41 was more serious than that over Pd/Beta-H; for example, after 90 min, pyrene conversion was 94% over Pd/Beta-H and 90% over Pd/Al-MCM-41 in the absence of sulfur and 87 and 57%, respectively, in the presence of 200-ppm sulfur. These results indicate the superior sulfur tolerance of Pd/Beta-H in pyrene hydrogenation.

Table 5 presents the product selectivities in pyrene hydrogenation over the Pd/Beta-H and Pd/Al-MCM-41 catalysts in the absence and presence of 200-ppm sulfur in the form of thiophene or 4,6-DMDBT at a reaction time of 180 min. Although pyrene conversion in the absence of sulfur (runs 1 and 4 in Table 5) was similar over the two catalysts, the selectivity for deep hydrogenation

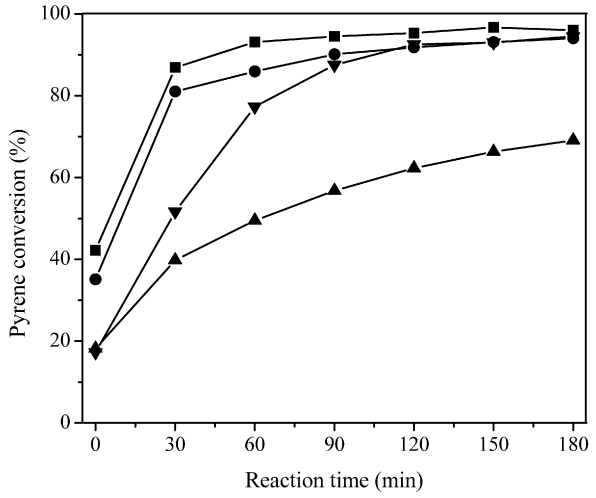

Fig. 10. Dependence of the pyrene conversion on reaction time in the absence and presence of 200-ppm sulfur in the form of thiophene. (■) Over Pd/Beta-H in the absence of sulfur; (●) over Pd/Al-MCM-41 in the absence of sulfur; (▼) over Pd/Beta-H in the presence of thiophene; (▲) over Pd/Al-MCM-41 in the presence of thiophene.

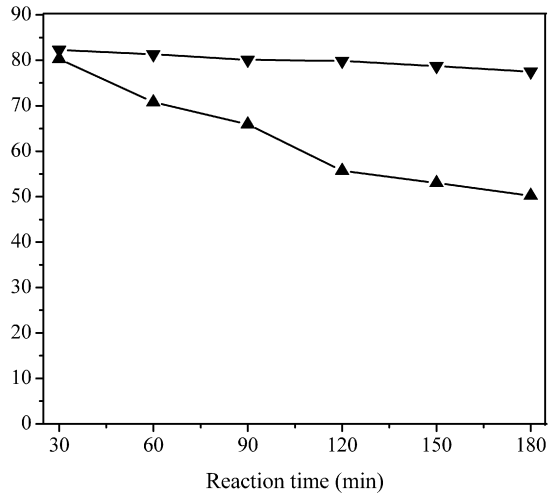

Fig. 11. Decreased percentages of DHP in pyrene hydrogenation versus reaction time after addition of 200-ppm sulfur in the form of thiophene. (▲) Over Pd/Beta-H; (▼) over Pd/Al-MCM-41.

products (the sum of hexahydropyrene, decahydropyrene, and perhydropyrene; DHP) over Pd/Beta-H was almost twice that of over Pd/Al-MCM-41, demonstrating Pd/Beta-H's much greater deep hydrogenation ability.

Furthermore, after addition of 200-ppm sulfur in the form of thiophene (runs 2 and 5 in Table 5), Pd/Beta-H still exhibited a much higher conversion rate for pyrene than Pd/Al-MCM-41 (94.5 vs 69.1%). Furthermore, the hydrogenation products dihydropyrene, tetrahydropyrene, hexahydropyrene, decahydropyrene, and perhydropyrene were observed over Pd/Beta-H, whereas only dihydropyrene, tetrahydropyrene, and hexahydropyrene were observed over Pd/Al-MCM-41. These findings indicate that DHP products were greatly suppressed over the two catalysts after the addition of 200-ppm sulfur in the form of thiophene.

In contrast, after addition of 200-ppm sulfur in the form of 4,6-DMDBT (runs 3 and 6 in Table 5), the conversion of pyrene and the DHP content were only slightly decreased, but the Pd/Beta-H still exhibited much greater catalytic activity than Pd/Al-MCM-41. Furthermore, comparing pyrene hydrogenation in the presence of thiophene with 4,6-DMDBT (Table 5) clearly showed that 4,6-DMDBT has less poisoning effect than thiophene. Generally, both

Table 5
Product selectivities in pyrene hydrogenation over Pd/Beta-H and Pd/Al-MCM-41 catalysts for reaction time of 180 min

Run	Catalyst	Pyrene conversion (%)	Product selectivity (%)							
			B	E	C	D	F	G	H	DHP[c]
1	Pd/Beta-H	96.3	10.5	24.2	24.9	6.2	11.8	10.7	8.1	61.6
2	Pd/Beta-H[a]	94.5	24.5	39.3	16.2	5.7	2.7	3.4	2.7	30.7
3	Pd/Beta-H[b]	95.2	12.9	27.5	23.1	5.8	9.9	9.5	6.5	54.8
4	Pd/Al-MCM-41	94.0	23.4	37.8	12.8	5.3	5.8	4.2	4.7	32.8
5	Pd/Al-MCM-41[a]	69.1	40.7	21.0	4.2	2.7	0	0	0	7.4
6	Pd/Al-MCM-41[b]	92.6	24.4	38.7	12.1	5.5	4.6	3.1	2.4	27.7

[a] The presence of 200-ppm sulfur in the form of thiophene.
[b] The presence of 200-ppm sulfur in the form of 4,6-DMDBT.
[c] The sum of C, D, F, G, and H (deep hydrogenation products, DHP).

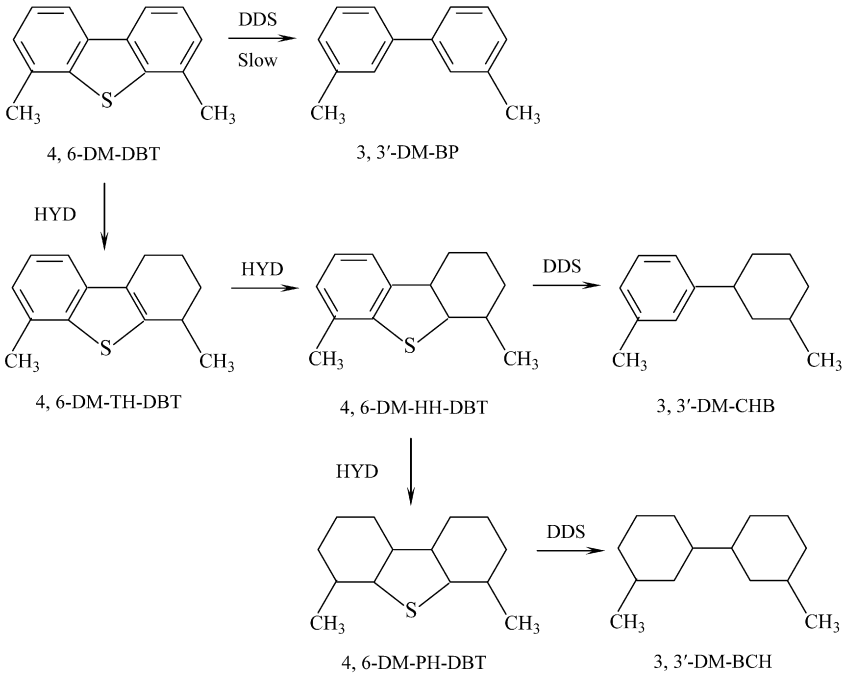

Fig. 12. Network of 4,6-DMDBT hydrodesulfurization.

thiophene and 4,6-DMDBT can be adsorbed on catalytically active sites, leading to poisoning of the catalysts; however, 4,6-DMDBT is more strongly adsorbed. In addition, under the same reaction conditions, the sulfur in the thiophene molecule is more readily hydrodesulfurized to H_2S; therefore, the concentration of H_2S in the reaction is relatively high, resulting in serious catalyst poisoning.

To quantitatively analyze the change in DHP products in the absence and presence of 200-ppm sulfur in the form of thiophene over the Pd/Beta-H and Pd/Al-CMC-41 catalysts, Fig. 11 illustrates the time dependence of the decrease in the percentage of DHP (i.e., the percentage of DHP difference before and after addition of sulfur). The decrease in the percentage of DHP was much smaller over Pd/Beta-H than over Pd/Al-MCM-41, indicating the much better sulfur tolerance of Pd/Beta-H. The difference in sulfur tolerance in pyrene hydrogenation over the two catalysts is also attributed to their different acidity, as was discussed earlier for naphthalene hydrogenation. In addition, the Beta-H support has the advantages of both microporosity and mesoporosity, and, of course, the palladium particles are located in the micropores as well as the mesopores (Fig. 2b). Due to pore size limitations, hydrogenation of the bulky pyrene molecule occurs only in the mesopores. The palladium sites located in the mesopores that are poisoned by adsorbed sulfur may possibly be partially recovered by spillover hydrogen coming from the micropores [2,50].

3.4. Hydrodesulfurization of 4,6-DMDBT

As a refractory compound of the dialkyldibenzothiophenes in fuels hydrotreated over supported metal sulfide catalysts [2,51], 4,6-DMDBT was hydrodesulfurized over Pd/Beta-H and Pd/Al-MCM-41. Fig. 12 shows the proposed network of 4,6-DMDBT hydrodesulfurization [52]. Compared with hydrogenation route (HYD), the rate for direct desulfurization (DDS) of 4,6-DMDBT is very slow [51,52]. In our experiments, the product of 3,3′-dimethylbiphenyl (3,3′-DM-BP) was undetectable, confirming the slow DDS rate. The hydrogenation of a phenyl ring of 4,6-DMDBT imparts flexibility to the methyl group, resulting in the formation of flexible intermediates with reduction of the steric hindrance, followed by desulfurization [51]. Figs. 13 and 14 illustrate the time dependence of 4,6-DMDBT conversion and the remaining sulfur content in the liquid phase over Pd/Beta-H and Pd/Al-MCM-41. The conversion of 4,6-DMDBT was lower over Pd/Beta-H than over Pd/Al-MCM-41 (Fig. 13), due to the larger number of exposed Pd atoms for 4,6-DMDBT in Pd/Al-MCM-41 (with Pd particles inside mesopores) compared with Pd/Beta-H (with Pd particles inside both mesopores and micropores). However, analysis of reactants and products by the sulfur analyzer demonstrated a much higher sulfur content remaining in the reaction system over Pd/Al-MCM-41 than over Pd/Beta-H (Fig. 14), indicating Pd/Beta-H's much greater desulfurization ability. As discussed earlier for the hy-

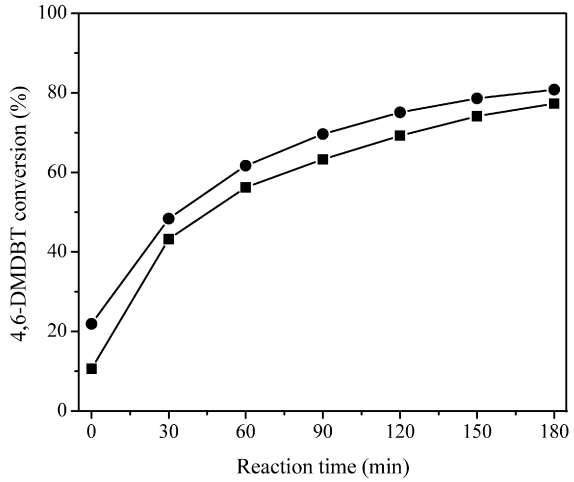

Fig. 13. Dependences of 4, 6-DMDBT conversions on reaction time. (■) Pd/Beta-H; (●) Pd/Al-MCM-41.

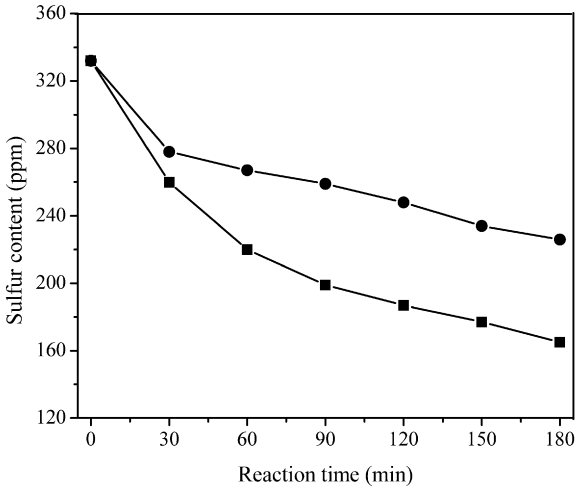

Fig. 14. Dependences of the remaining sulfur content in 4,6-DMDBT-hydrogenation system on reaction time. (■) Pd/Beta-H; (●) Pd/Al-MCM-41.

drogenation of naphthalene and pyrene, because of Pd/Beta-H's superior hydrogenation ability, deep hydrogenation or C-S bond-breaking of 4,6-DMDBT, which facilitates the HDS of 4,6-DMDBT, occurred more readily on Pd/Beta-H than on Pd/Al-MCM-41. For example, when the reaction time reached 180 min, the sulfur content in the liquid phase was 165 ppm over Pd/Beta-H, compared with 226 ppm over Pd/Al-MCM-41. These results indicate Pd/Beta-H's higher activity for hydrodesulfurization of 4,6-DMDBT. Recently, Lee et al. [53] reported the HDS of 4,6-DMDBT over Co-MoS catalysts supported on nanoporous carbon. They obtained a 4,6-DMDBT conversion of 55.4% at 4.0 MPa, 320 °C, and a reaction time of 240 min in an autoclave. In our case, under mild conditions (6.5 MPa, 250 °C, 180 min), the Pd/Beta-H catalyst demonstrated a 4,6-DMDBT conversion of 77%. These results confirmed that nobel metal catalysts supported on acidic mesoporous zeolites are very helpful for the deep HDS of 4,6-DMDBT.

To gain insight into the difference in catalytic activity for the HDS of 4,6-DMDBT, we analyzed the products catalyzed by Pd/Beta-H and Pd/Al-MCM-41 by GC-MS, and obtained the following results:

1. Such compounds as 4,6-dimethyl-1,2,3,4-tetrahydrodibenzothiophene (4,6-DM-TH-DBT), 4,6-dimethyl-1,2,3,4,4a,9b-hexadibenzothiophene (4,6-DM-HH-DBT), 4,6-dimethylperhydrodibenzothiophene (4,6-DM-PH-DBT), and 3,3′-dimethylbicyclohexyl (3,3′-DM-BCH) [52,54–56] were formed over Pd/Al-MCM-41. 4,6-DM-TH-DBT, 4,6-DM-HH-DBT, and 4,6-DM-PH-DBT were the intermediates in the hydrogenation of 4,6-DMDBT, and 3,3′-DM-BCH resulted from the hydrodesulfurization of 4,6-DM-PH-DBT [54,56], suggesting that the hydrodesulfurization of 4,6-DMDBT over Pd/Al-MCM-41 occurred via the HYD pathway. This finding is in good agreement with the results obtained for Pd/γ-Al_2O_3 and Pt-Pd/γ-Al_2O_3 reported previously [54–56].
2. In addition to 4,6-DM-TH-DBT, 4,6-DM-HH-DBT, and 4,6-DM-PH-DBT, we found a significant amount of light hydrocarbons (C_5–C_9) over Pd/Beta-H, which may be hydrocracking products of intermediates formed from 4,6-DMDBT. In particular, we found cyclohexane, suggesting that demethylation and scission of the C–C bond connecting the two rings in cyclohexylbenzene may occur over Pd/Beta-H.
3. The difference in the products between Pd/Beta-H and Pd/Al-MCM-41 also is related to the change in the Beta-H zeolite and Al-MCM-41 supports, because the palladium loadings and particle sizes are almost the same for the two catalysts. The higher acidity is favorable for demethylation and scission of the C–C bond connecting the two rings [51]. Similar phenomena have been reported over alumina-supported CoMo and NiMo catalysts modified by acidic zeolites [33,34] and by the addition of phosphorus and fluorine [36–38].

Recently, Niquille-Röthlisberger and Prins [57,58] compared the catalytic activity in HDS of 4,6-DMDBT over Pd supported on amorphous silica-alumina (ASA) and over alumina and found that the ASA-supported Pd catalyst had a much higher activity than the alumina-supported Pd catalyst. They have suggested that the more strongly acidic ASA support is beneficial for the creation of electron-deficient Pd particles, leading to better sulfur resistance and improved hydrogenation properties [57]. This was further confirmed by catalytic results in the presence of pyridine and piperidine [58]. In addition, Niquille-Röthlisberger and Prins suggested that a new reaction might occur: hydrogenation by spillover of hydrogen atoms to 4,6-DMDBT molecules adsorbed on the support in the vicinity of the Pd particles [57]. In our case, compared with Al-MCM-41, the strongly acidic Beta-H support may have an advantage in the creation of electron-deficient Pd particles and the adsorption of 4,6-DMDBT molecules on acidic sites near the Pd particles [57], leading to significantly improved catalyst activity.

4. Conclusion

Compared with Pd/Al-MCM-41, Pd/Beta-H exhibited good sulfur tolerance in the hydrogenation of naphthalene and pyrene and greater activity in the HDS of 4,6-DMDBT. These findings are attributed to the differing support acidity of Beta-H zeolite and Al-MCM-41.

Acknowledgments

This work was supported by the State Basic Research Project of China (grant 2004CB217804) and the National Natural Science Foundation of China (grants 20573044 and 20773049).

References

[1] A. Stanislaus, B.H. Cooper, Catal. Rev. Sci. Eng. 36 (1994) 75.
[2] C. Song, X.L. Ma, Appl. Catal. B 41 (2003) 207.
[3] C. Song, Catal. Today 86 (2003) 211.
[4] J. Barbier, E. Lamy-Pitara, P. Marecot, J.P. Boitiaux, J. Cosyns, F. Verna, Adv. Catal. 37 (1990) 279.
[5] B.H. Cooper, B.L. Donnis, Appl. Catal. A 137 (1996) 203.

[6] C. Song, A.D. Schmitz, Energy Fuels 11 (1997) 656.
[7] H. Yasuda, N. Matsubayashi, T. Sato, Y. Yoshimura, Catal. Lett. 54 (1998) 23.
[8] H. Yasuda, T. Sato, Y. Yoshimura, Catal. Today 50 (1999) 63.
[9] B. Pawelec, R. Mariscal, R.M. Navarro, S. van Bokhorst, S. Rojas, J.L.G. Fierro, Appl. Catal. A 225 (2002) 223.
[10] J.T. Miller, D.C. Koningsberger, J. Catal. 162 (1996) 209.
[11] W.M.H. Sachtler, A.Y. Stakheev, Catal. Today 12 (1992) 283.
[12] S.D. Lin, M.A. Vannice, J. Catal. 143 (1993) 539.
[13] S.D. Lin, M.A. Vannice, J. Catal. 143 (1993) 563.
[14] S.D. Lin, M.A. Vannice, J. Catal. 143 (1993) 554.
[15] L.J. Simon, J.G. van Ommen, A. Jentys, J.A. Lercher, J. Phys. Chem. B 104 (2000) 11644.
[16] L.J. Simon, J.G. van Ommen, A. Jentys, J.A. Lercher, J. Catal. 201 (2001) 60.
[17] L.J. Simon, J.G. van Ommen, A. Jentys, J.A. Lercher, J. Catal. 203 (2001) 434.
[18] A.H. Janssen, A.J. Koster, K.P. de Jong, Angew. Chem. Int. Ed. 40 (2001) 1102.
[19] A.H. Janssen, A.J. Koster, K.P. de Jong, J. Phys. Chem. B 106 (2002) 11905.
[20] S. van Donk, A.H. Janssen, J.H. Bitter, K.P. de Jong, Catal. Rev. 45 (2003) 297.
[21] T.D. Tang, C.Y. Yin, L.F. Wang, Y.Y. Ji, F.S. Xiao, J. Catal. 249 (2007) 111.
[22] F.-S. Xiao, L.F. Wang, C.Y. Yin, K.F. Lin, Y. Di, J.X. Li, R.R. Xu, D.S. Su, R. Schlögl, T. Yokoi, T. Tatsumi, Angew. Chem. Int. Ed. 45 (2006) 3090.
[23] H. Wang, T.J. Pinnavaia, Angew. Chem. Int. Ed. 45 (2006) 7603.
[24] M. Choi, H. Cho, R. Srivastava, C. Venkatesan, D. Choi, R. Ryoo, Nat. Mater. 5 (2006) 718.
[25] R. Srivastava, M. Choi, R. Ryoo, Chem. Commun. (2006) 4489.
[26] T. Fujikawa, O. Chiyoda, M. Tsukagoshi, K. Idei, S. Takehara, Catal. Today 45 (1998) 307.
[27] K.G. Knudsen, B.H. Cooper, H. Topsøe, Appl. Catal. A 189 (1999) 205.
[28] H. Schulz, W. Böhringer, P. Waller, F. Ousmanov, Catal. Today 49 (1999) 87.
[29] C. Li, Z.X. Jiang, J.B. Gao, Y.X. Yang, S.J. Wang, F.P. Tian, F.X. Sun, X.P. Sun, P.L. Ying, C.R. Han, Chem. Eur. J. 10 (2004) 2277.
[30] M.V. Landau, Catal. Today 36 (1997) 393.
[31] V. Meille, E. Schulz, M. Lemaire, M. Vrinat, J. Catal. 170 (1997) 29.
[32] F. Bataille, J.L. Lemberton, P. Michaud, G. Pérot, M. Vrinat, M. Lemaire, E. Schulz, M. Breysse, S. Kasztelan, J. Catal. 191 (2000) 409.
[33] M.V. Landau, D. Berger, M. Herskowitz, J. Catal. 159 (1996) 236.
[34] T. Isoda, S. Nagao, X.L. Ma, Y. Korai, I. Mochida, Energy Fuels 10 (1996) 1078.
[35] E. Lecrenay, K. Sakanishi, I. Mochida, Catal. Today 39 (1997) 13.
[36] E. Lecrenay, K. Sakanishi, I. Mochida, T. Suzuka, Appl. Catal. A 175 (1998) 237.
[37] C. Kwak, M.Y. Kim, K. Choi, S.H. Moon, Appl. Catal. A 185 (1999) 19.
[38] C. Kwak, J.J. Lee, J.S. Bae, K. Choi, S.H. Moon, Appl. Catal. A 200 (2000) 233.
[39] I.I. Abu, K.J. Smith, J. Catal. 241 (2006) 356.
[40] I.I. Abu, K.J. Smith, Appl. Catal. A 328 (2007) 58.
[41] A.J. Wang, L.F. Ruan, Y. Teng, X. Li, M.H. Lu, J. Ren, Y. Wang, Y.K. Hu, J. Catal. 229 (2005) 314.
[42] X. Li, A.J. Wang, S. Zhang, Y.Y. Chen, Y.K. Hu, Appl. Catal. A 316 (2007) 134.
[43] X.C. Meng, Y.X. Wu, Y.D. Li, J. Porous Mater. 13 (2006) 365.
[44] H.J. Zhang, X.C. Meng, Y.D. Li, Y.S. Lin, Ind. Eng. Chem. Res. 46 (2007) 4186.
[45] L.Y. Chen, Z. Ping, G.K. Chuah, S. Jaenicke, G. Simon, Micro. Meso. Mater. 27 (1999) 231.
[46] J.J.F. Scholten, A.P. Pijpers, A.M.L. Hustings, Catal. Rev. Sci. Eng. 27 (1985) 151.
[47] W.M. Zhang, P.G. Smirniotis, M. Gangoda, R.N. Bose, J. Phys. Chem. B 104 (2000) 4122.
[48] A. Corma, A. Martínez, V. Martínez-Soria, J. Catal. 169 (1997) 480.
[49] T.C. Huang, B.C. Kang, Ind. Eng. Chem. Res. 34 (1995) 1140.
[50] C. Song, CHEMTECH 29 (1999) 26.
[51] S.K. Bej, S.K. Maity, U.T. Turaga, Energy Fuels 18 (2004) 1227.
[52] M. Egorova, R. Prins, J. Catal. 224 (2004) 278.
[53] J.J. Lee, S. Han, H. Kim, J.H. Koh, T. Hyeon, S.H. Moon, Catal. Today 86 (2003) 141.
[54] A. Niquille-Röthlisberger, R. Prins, J. Catal. 235 (2005) 229.
[55] P. Kukula, V. Gramlich, R. Prins, Helv. Chim. Acta 89 (2006) 1623.
[56] A. Niquille-Röthlisberger, R. Prins, J. Catal. 242 (2006) 207.
[57] A. Niquille-Röthlisberger, R. Prins, Catal. Today 123 (2007) 198.
[58] A. Niquille-Röthlisberger, R. Prins, Ind. Eng. Chem. Res. 46 (2007) 4124.